# Ultrafast vibrational dynamics and spectroscopy of a siloxane self-assembled monolayer

Satoshi Nihonyanagi,[a] Ali Eftekhari-Bafrooei, and Eric Borguet[b]
*Department of Chemistry, Temple University, Philadelphia, Pennsylvania 19122, USA*

(Received 9 August 2010; accepted 1 November 2010; published online 22 February 2011)

Time and frequency domain sum-frequency generation (SFG) were combined to study the dynamics and structure of self-assembled monolayers (SAMs) on a fused silica surface. SFG-free induction decay (SFG-FID) of octadecylsilane SAM in the CH stretching region shows a relatively long time scale oscillation that reveals that six vibrational modes are involved in the response of the system. Five of the modes have commonly been used for the fitting of SFG spectra in the CH stretching region, namely the symmetric stretch and Fermi resonance of the methyl group, the antisymmetric stretch of the methyl, as well as the symmetric and antisymmetric stretches of the methylene group. The assignment of the sixth mode to the terminal $CH_2$ group was confirmed by performing a density function theory calculation. The SFG-FID measures the vibrational dephasing time ($T_2$) of each of the modes, including a specific $CH_2$ group within the SAM, the terminal $CH_2$, which had never been measured before. The relatively long (~1.3 ps) dephasing of the terminal $CH_2$ suggests that alkyl monolayer structure is close to that of the liquid condensed phase of Langmuir Blodgett films.
 [doi:10.1063/1.3518457]

## I. INTRODUCTION

Self-assembly of molecular films from solution has been extensively employed to construct thin organic monolayers because a molecularly ordered structure with a wide variety of functionalities can be prepared very easily and without the expensive and sophisticated equipment essential for organic layer formation in ultrahigh vacuum.[1] The diverse applications of molecular self-assembly range from simple corrosion resistant layers to more complex integrated functionalities such as organic light emitting diodes[2,3] and molecular electronics.[4,5] As many applications depend on the degree of molecular ordering, it is also important to develop methods to analyze surface structures.

Sum frequency generation (SFG) spectroscopy, a second-order nonlinear optical technique, provides excellent surface specificity and structure sensitivity based on the symmetry restriction that systems with local inversion centers cannot generate SFG.[6] SFG has become a powerful tool to investigate structures of interfacial molecules.[7,8] SFG spectroscopy with ultrashort laser pulses can also be applied for probing the ultrafast surface dynamics.[9–12] For example, the vibrational population relaxation time ($T_1$) and vibrational dephasing time ($T_2$) of surface species can be measured by time domain SFG.[13] A number of frequency domain SFG measurements, i.e., SFG spectroscopy, have been reported for various interfaces[14–17] since the first reported application of this technique.[18] However, obtaining dynamics information from frequency domain spectroscopy is not trivial. Furthermore, frequency domain spectroscopy is often congested by overlapping vibrational modes, making it difficult to identify, assign and analyze each of the features contributing to the spectrum.

Time domain SFG measurements, e.g., SFG free induction decay (SFG-FID), offer an alternative way to measure the same parameters as are obtained from frequency domain measurements. However, different features are emphasized in FID as compared to spectroscopy measurements as is known from the comparisons of time- and frequency-domain NMR[19] or Electron Paramagnetic Resonance[20] spectroscopy. Some features which are not clear in the frequency domain could be clearer in time domain measurements.

The first SFG-FID measurement was reported by Guyot-Sionnest in 1991 from Si-H vibration on a hydrogen terminated silicon (111) surface.[21] SFG-FID of other systems, such as CO on a metal surface,[22–25] and of Langmuir Blodgett (LB) films on insulators[26,27] has been reported.

In the present investigation, we have studied the SFG-FID and SFG spectra of octadecylsilane (ODS) on a fused silica surface at the C-H stretching region. The SFG-FID is characterized by a long coherence that is shown to involve six frequency components as demonstrated by the simultaneously fit the SFG-FID and SFG spectra. Details of the fitting process and mode assignment are discussed. Density function theory (DFT) calculations help to assign one of the modes to a terminal $CH_2$. The possible correlation of the structure of ODS self-assembled monolayers (SAMs) to the dephasing of the different oscillators is discussed.

## II. EXPERIMENTAL

All glassware and the IR grade fused silica prism (IRFS, ISP optics) were cleaned by piranha solution [3:1(v/v), concentrated sulfuric acid and 30% hydrogen peroxide

[a]Present address: Molecular Spectroscopy Laboratory, Advanced Science Institute, RIKEN, 2-1 Hirosawa, Wako, Saitama 351-0198, Japan.
[b]Author to whom correspondence should be addressed. Electronic mail: eborguet@temple.edu.

 

(*Caution! Piranha solution is a very strong oxidant and is extremely dangerous to work with; gloves, goggles, and a face shield should be worn*)] and dried by a stream of hot air prior to use. ODS monolayers were prepared by immersing the clean IR fused silica prism for 20 min into 2.5 mM octadecyltrichlorosilane (Gelest Inc.) solution in (4:1) hexadecane (Sigma, >99%) and $CHCl_3$ (Sigma Aldrich, 99.8%).[28–30] The ODS coated prism was rinsed with $CHCl_3$ and air dried.

A femtosecond regenerative amplifier (Quantronix, Integra-E), seeded by a Ti:sapphire oscillator (Coherent, Mira seed), produces 3.5 mJ laser pulses centered at 815 nm with a duration of ~100 fs at a repetition rate of 1 kHz. 90% of the regenerative amplifier energy was employed to pump an optical parametric amplifier (Light Conversion, TOPAS) which generates tunable IR radiation (1180–2640 nm) with a total power (signal and idler) of 900 mW at the peak. Mid-infrared radiation was obtained by difference frequency generation in an $AgGaS_2$ crystal with a peak power of 30 $\mu$J at 3 $\mu$m. The remaining 10% of the regenerative amplifier output was used as the visible light for SFG measurements. The energy and polarization of the visible beam were adjusted by a combination of a half-wave plate and a prism polarizer. The IR bandwidth is ~130 $cm^{-1}$ FWHM.

For frequency domain SFG measurements, the visible pulse was spectrally narrowed to a FWHM of ~0.9 nm (14 $cm^{-1}$) by a pair of band-pass filters (CVI) Fig. 1(a). The visible and infrared beams, with energies of ~2 $\mu$J/pulse and ~10 $\mu$J/pulse, respectively, were overlapped in time and space at the sample surface. The spot diameters, at the sample, of the visible and IR beams were ~0.2 mm and ~0.4 mm, respectively. The incident angles of the visible and infrared light were about 65° and 55°, respectively. The time delay between IR and visible beams was adjusted so that the SFG intensity was maximized. The SFG signal was separated from the reflected visible light by short pass filters (Melles Griot) and was detected by a CCD detector (Princeton Instruments) coupled with a polychromator (300i, Acton Research Corp.). In the experiments reported here, the SFG, visible, and IR beams were polarized *s, s,* and *p*, respectively. The SFG measurements were carried out in air at room temperature (~23 °C, 20% relative humidity).

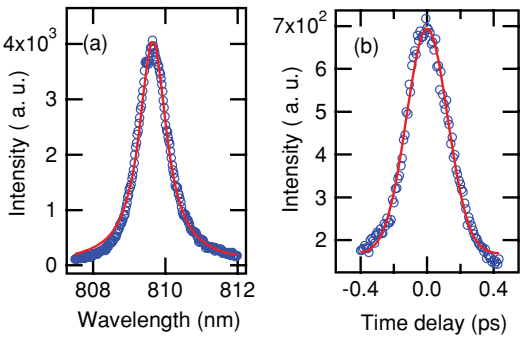


FIG. 1. Characterization of pulses used in the present study. (a) Spectrum of narrowband visible light used in frequency domain measurement (open circle), which determines the spectral resolution. The spectral line shape is determined by the interference filter. The solid line is a Lorentzian fit to the data. The FWHM is 0.9 nm (14 $cm^{-1}$). (b) Cross correlation of infrared and visible (without narrowband filter) pulses, which determines the temporal resolution in time domain measurement. The solid line shows a Gaussian fit.

For time domain measurement, the band-pass filter is replaced by a neutral density filter to attenuate the visible intensity. In this way, the change of the optical path between the time and frequency domain measurements is minimized. The $t = 0$ was set to be the cross-correlation maxima obtained from gold coated prism, within an experimental error of ± ~0.1 ps. Accordingly, the $t = 0$ was allowed to vary ± 0.1 ps in the fitting process (see Sec. III). The time domain system response function was determined to be ~190 fs FWHM from the cross-correlation measure on a gold film evaporated on a IRFS prism under the same experimental geometry as ODS coated IRFS, i.e., total internal reflection, assuming Gaussian temporal profiles for the visible and IR pulses [Fig. 1(b)].

Data analysis and curve fitting was realized by custom written programs using a commercial software (Wave Metrics, Igor Pro). The square root of the SFG intensity was used as a weighting function to determine the goodness of fit as judged from the reduced chi-squared DFT calculations were performed using the B3LYP level of theory with the 6-31G(*d,p*) basis set contained in GAUSSIAN 03 (Revision C.02, Gaussian, Inc., Wallingford CT, 2004).

## III. RESULTS AND DISCUSSION

The SFG-FID of the ODS SAM in the C-H stretching region shows relatively long coherence accompanied with oscillations that persist for over 1 ps [Fig. 2(a)]. The first peak in the FID appears at ~0.1 ps, and not at 0.0 ps, because of the finite duration of the infrared excitation pulse. The oscillation in the SFG-FID is caused by interference between the multiple oscillators which alternately beat in phase and out of phase in time due to the mismatch of their natural frequencies. The Fourier transform of the oscillatory components in the FID is also shown in the inset of Fig. 2(a). The Fourier power spectrum shows a peak at ~60 $cm^{-1}$, which corresponds to the peak separation of two major peaks due to methyl stretching modes in the frequency domain spectrum [see Fig. 2(b)] and the oscillation period of the FID trace (0.6 ps). For a quantitative analysis, the spectrum and FID trace were simultaneously fit to Eqs. (1) and (2a), assuming a variable number of vibrational modes in the CH stretching region as discussed in the following section.

### A. Fitting

A number of reviews have been published describing the theoretical background of SFG and its applications.[6,8,14] SFG is a second-order nonlinear optical processes in which two photons at frequencies of $\omega_1$ and $\omega_2$ generate one photon of frequency $\omega_3 = \omega_1 + \omega_2$. Second-order nonlinear optical processes, including SFG, do not take place in media with inversion symmetry under the electric dipole approximation but do occur at interfaces, where the inversion symmetry is necessarily broken. For the IR-visible SFG spectroscopy, three types of measurements have been employed, i.e.,

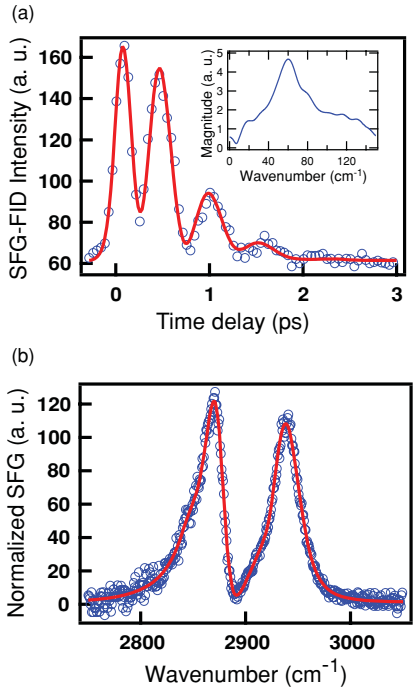


FIG. 2. SFG FID (a) and normalized SFG spectrum; (b) of ODS SAM. The open circles represent the experimentally observed SFG signals with simultaneous fit curves using six frequency components represented by red solid lines, respectively. Inset of (a) shows the Fourier transform of the oscillatory components in the FID trace which is obtained by subtracting a double exponential decay fit to the FID trace. The SFG spectrum was normalized by dividing the raw spectrum of the OTS sample by a spectrum obtained from a sample of GaAs (arbitrarily scaled).

scanning narrowband IR, broadband IR,[31] and FT-SFG.[32] Here, we employed broadband SFG system because of the convenience of switching between the time- and frequency-domain measurements. The frequency domain SFG intensity generated by a broadband IR pulse can be expressed as a modification of the well-known SFG equation:[15,27,33]

$$I_{\mathrm{SFG}} \propto \left| \sum_n \frac{A_n}{\omega_{\mathrm{IR}} - \omega_n + i(\Gamma_n + \Delta\omega_{\mathrm{vis}}/2)} + \frac{|A_{\mathrm{NR}}|}{\Delta\omega_{\mathrm{IR}}} e^{i\varepsilon} \right|^2 \times \exp\left\{ -\left( \frac{\omega_{\mathrm{IR}} - \omega_0}{\Delta\omega_{\mathrm{IR}}} \right)^2 \right\} \quad (1)$$

where $\omega_{\mathrm{IR}}$ is the frequency of the incident IR light and $A_{\mathrm{NR}}$, $\varepsilon$, $A_n$, and $\Gamma_n$ are the vibrationally nonresonant susceptibility component, the phase between the resonant and nonresonant contributions, the amplitude and damping constant of the surface vibration with frequency $\omega_n$, respectively. $\varepsilon$ is often set to be a free variable. However, according to electromagnetic theory $\varepsilon$ must be zero for electronically nonresonant substrate such as silica glass. Indeed, nonresonant phases for silica glass and water surfaces were determined to be zero in phase sensitive measurements.[34,35] Thus, $\varepsilon$ is fixed to be zero in the present fitting. The exponential term describes the Gaussian shaped spectrum of the incident IR pulse, where $\omega_0$ and $\Delta\omega_{\mathrm{IR}}$ represent the center frequency and spectral width of the IR pulse, respectively. $A_{\mathrm{NR}}$ is divided by $\Delta\omega_{\mathrm{IR}}$ because the nonresonant polarization spreads over the whole spectral region in the frequency domain measurement while it is summed up in the time domain measurement. As the spectral resolution of the SFG spectrum is limited to 14 $\mathrm{cm}^{-1}$, by the bandwidth of the visible pulse ($\Delta\omega_{\mathrm{vis}}$), the full widths at half maxima ($2\Gamma$) of the vibrational bands determined from the spectrum are broadened by the limited resolution of the spectral measurement. The Benderskii group took this into account by deconvoluting a Gaussian spectral shape from the measured spectra.[27] Alternatively, $\Delta\omega_{\mathrm{vis}}/2$ is simply added to $\Gamma_n$, i.e., $\Gamma \sim \Gamma_n + \Delta\omega_{\mathrm{vis}}/2$ because the interference filter gives a rather Lorenzian line shape [Fig. 1(a)]. Here, the Fresnel factors and prefactors are ignored as they are the same in all the experiments.

In the SFG-FID measurement, a short IR pulse creates a coherent superposition of vibrational modes and a short, time-delayed visible pulse probes the remaining coherence by generating a response at the sum-frequency as a function of the time delay. Since the FID and spectrum are related to each other by Fourier transform, the FID and spectroscopy measurements, in principle, should contain identical information. In practice, however, because the time domain measurement, as long as it captures all of the response, is free from spectral resolution limitations, the FID measurement allows us to determine the vibrational linewidth with better spectral resolution than the frequency domain measurement. In other words, because the SFG spectrum is taken with short pulses ($\tau_{\mathrm{vis}} \sim 0.6$ ps and $\tau_{\mathrm{IR}} \sim 0.1$ ps) it undersamples the vibrational modes that have long dephasing times. This is demonstrated in the Fourier transformation of the spectrum shown in Fig. 3 (black line) where the FFT of the spectrum decays faster than the FID measured in time domain. On the other hand, measurement in the frequency domain is advantageous to probe spectrally broad (temporally sharp) feature, i.e., the only way for a time domain experiment to faithfully reproduce a spectrally broad feature is to measure its response in the time domain with a very short pulse.[36]

The theory of time domain SFG measurement has been described by Mii and Ueba[37,38] Following the Benderskii[27] and Bonn groups,[39] the SFG intensity as a function of

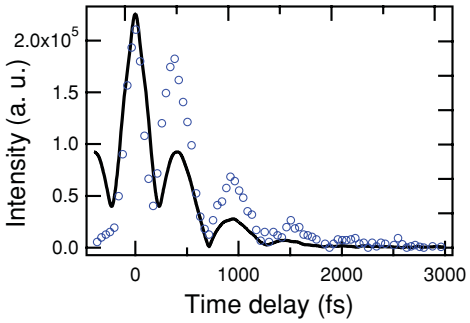


FIG. 3. FFT of the ODS spectrum (black) and the measured FID (blue). The FID trace was arbitrarily scaled so that the first peak has about the same amplitude as FFT. The more rapid decay of the FFT of the ODS spectrum is a consequence of the undersampling of modes with long dephasing times. This demonstrates the effect of a finite nonzero $\Delta\omega_{\mathrm{vis}}/2$ in Eq. (1).

delay time ($t_d$) between IR and visible pulses can be written as follows:

$$I_{\text{SFG-FID}}(t_d) \propto \int_{-\infty}^{\infty} dt \left| P^{(2)}(t, t_d) \right|^2, \tag{2a}$$

$$P^{(2)}(t, t_d) \propto E_{\text{vis}}(t - t_d)\, P^{(1)}(t), \tag{2b}$$

$$P^{(1)}(t) = \int_{-\infty}^{\infty} dt' E_{\text{IR}}(t - t') S(t'), \tag{2c}$$

$$S(t) = \left[ \delta(t) |A_{NR}| \exp(i\varepsilon) - i\theta(t) \sum_n A_{R,n} \times \exp\{2\pi c(-i\omega_n t - \Gamma_n t)\} \right] + \text{c.c.} \tag{2d}$$

The time response function, $S(t)$, of the system is given by Eq. (2d) where $\delta(t)$ is the delta function, $\theta(t)$ is the Heaviside step function, $c$ is the speed of light and the inverse of $2\pi c\Gamma_n$ is the total dephasing time of $n$th vibrational mode ($T_{2,n}$) and is ~5.3 ps /$\Gamma_n$ when $\Gamma_n$ is expressed in cm$^{-1}$. [Note that the bandwidth (FWHM) is given by 2$\Gamma$.] The first order polarization induced by the IR excitation pulse [Eq. (2c)] is mixed with the polarization induced by the visible pulse, creating the second-order polarization [Eq. (2b)]. The two integrations in Eqs. (2a) and (2c) are required to consider the finite pulse width of the incident IR and visible beams. The pulse shapes are assumed to be Gaussian:

$$E_{\text{IR/Vis}}(t) = E_{\text{IR/Vis}} \exp\left(-t^2/\tau^2 - i2\pi c\omega_{\text{IR/Vis}} t\right) + \text{c.c.}, \tag{3a}$$

$$\bar{E}_{\text{IR}}(\omega) = \bar{E}_{\text{IR}} \exp\left(-(\omega - \omega_0)^2/\Delta\omega_0^2\right), \tag{3b}$$

where, $E_{\text{IR/vis}}$ denotes the magnitude of $E(t)$ for either IR or visible and $\tau$ is the pulsewidth. Using Eqs. (2d) and (3), Eq. (2c) can be written as follows:

$$P^{(1)}(t) = P_{\text{NR}}^{(1)}(t) + P_R^{(1)}(t) + \text{c.c.}, \tag{4a}$$

$$P_{\text{NR}}^{(1)}(t) = |A_{\text{NR}}| \exp(-t^2/\tau^2 + i\varepsilon - i2\pi c\omega_0 t), \tag{4b}$$

$$P_R^{(1)}(t) = -\int_{-\infty}^{t} e^{-(t'^2/\tau^2)} dt' \sum_n i A_{R,n} \times \exp\left[-\left\{(\omega_n - \omega_0)^2/\Delta\omega_{\text{IR}}^2\right\}\right] \times \exp\{2\pi c(-i\omega_n t - \Gamma_n t)\}. \tag{4c}$$

Here, we assume that the dephasing time of each vibrational mode is longer than the pulse width so that the decay part in Eq. (4c) is independent of the pulse width. In modeling the FID measurements, Eq. (4c) accounts for the Gaussian shaped spectral profile of the IR excitation pulse. The amplitude, $A_R$, is multiplied by the Gaussian shaped spectrum (center wavenumber $\omega_0 = 2900$ cm$^{-1}$ and $\Delta\omega_{\text{IR}} = 80$ cm$^{-1}$, corresponding to a FWHM of 133 cm$^{-1}$).

The fitting of the SFG-FID is extremely sensitive to the position of time zero, the position of maximum overlap between visible and IR pulses. The maxima of the FID trace actually appears at a time later than the zero time determined by the cross correlation maximum, by typically by 0.1 ps. This is because of the noninstantaneous build up of the resonant polarization.[37,38] This expressed by the integration (known as error function) in Eq. (4). In addition, an experimental error may possibly occur when a sample is replaced by the reference sample (gold film) for the cross-correlation measurement. To address this source of error, $t$ in Eq. (4) is replaced by $(t-t_0)$ and $t_0$ is treated as a variable. As an illustration of the critical role of $t_0$, Fig. 4 shows the same FID trace as shown in Fig. 2 but with fitting curves with different fixed value of $t_0$. The results show that unless $t_0$ is fixed at values near the maximum of FID, the fit is poor.

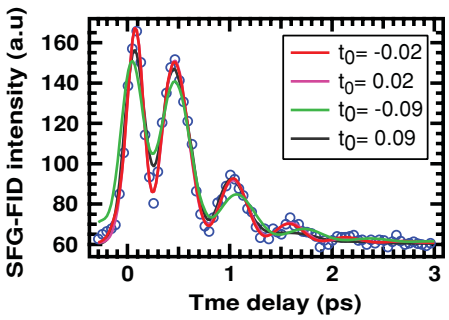


FIG. 4. The same SFG FID as shown in Fig. 2 (open circles). The lines represent the fit curves assuming two frequency components with different fixed values of $t_0$.

The spectrum and FID were simultaneously fit using Eqs. (1)–(4). Although two components roughly reproduce the FID and the spectrum, a simultaneous fit of spectrum and FID allows us to resolve spectral features in more detail. The quantitative fit requires that the contributions of a larger number of modes be included. Increasing the number of frequency components improves the reduced $\chi^2$ value as tabulated in Table I. The best fit curves obtained with six vibrational modes are shown in Fig. 2. We note that a separate fitting of either the spectrum or the FID cannot produce an acceptable size of the fit uncertainty due to the large number of fit parameters. The simultaneous fit of the spectrum and the FID significantly reduces the uncertainty of the fit parameters. The assignment of the vibrational modes identified is discussed below.

## B. Assignment of peaks

Two major frequency components at 2872 and 2938 cm$^{-1}$ have been assigned to the symmetric stretch and Fermi resonance of the methyl ($r^+$ and $r^+_{\text{FR}}$).[40–43] Three additional frequency components at 2849, 2918, and 2970 cm$^{-1}$

TABLE I. The reduced chi squared [$\chi^2_{\text{red}} = \chi^2$/(number of data points − number of free variables)] obtained from SIMULTANEOUS fitting of the ODS spectrum and FID with 2, 3, 5, and 6 frequency components.

| Number of modes | $\chi^2_{\text{red}}$ | Modes included |
|---|---|---|
| 2 | 0.95 | $r^+$, $r^+_{\text{FR}}$ |
| 3 | 0.46 | $r^+$, $t$-$d^-$, $r^+_{\text{FR}}$ |
| 5 | 0.78 | $d^+$, $r^+$, $d^-$, $r^+_{\text{FR}}$, $r^-$ |
| 6 | 0.39 | $d^+$, $r^+$, $t$-$d^-$, $d^-$, $r^+_{\text{FR}}$, $r^-$ |

TABLE II. Parameters obtained from the frequency- and time-domain SFG measurements of the ODS SAM. The amplitude parameter $A_n$ and $|A_{NR}|$ are given in a relative scale with respect to the $r^+$ mode. Note that the bandwidth (FWHM) is given by $2\Gamma$. $T_2$ values are calculated from $\Gamma$.

| Mode | $\omega$ ($cm^{-1}$) | $A$ (a.u.) | $\Gamma$ ($cm^{-1}$) | $T_2$ (ps) |
|---|---|---|---|---|
| $d^+$ | $2849 \pm 2$ | $0.09 \pm 0.07$ | $3 \pm 4$ | 1.8 |
| $r^+$ | 2872 | 1.00 | $8 \pm 2$ | 0.66 |
| $t$-$d^-$ (0) | $2884 \pm 1$ | $-0.34 \pm 0.11$ | $4 \pm 2$ | 1.3 |
| $d^-(\pi)$ | $2918 \pm 14$ | $0.21 \pm 0.44$ | $15 \pm 23$ | 0.35 |
| $r^+_{FR}$ | $2938 \pm 1$ | $0.75 \pm 0.33$ | $7 \pm 2$ | 0.76 |
| $r^-$ | $2970 \pm 3$ | $-0.17 \pm 0.11$ | $10 \pm 7$ | 0.53 |
| $\lvert\chi_{NR}\rvert$ (a.u.) | $-0.47$ | | | |
| $\phi^{NR}$ (rad) | 0 | | | |
| $t_0$ | 0.004 | | | |

have been assigned to the symmetric ($d^+$) and antisymmetric ($d^-(\pi)$) stretch of the methylene, and antisymmetric stretch of the methyl ($r^-$) groups.[40–43] The fact that the amplitude of the $d^+$ and $d^-(\pi)$ peaks are small implies that the ODS molecules in the monolayer are essentially in an all-trans conformation, where the vibrations due to $CH_2$ groups are SFG inactive due to local inversion symmetry. The sixth vibrational mode at 2884 $cm^{-1}$ has been often neglected but its amplitude is larger than the amplitude of the $d^+$, $d^-(\pi)$, and $r^-$ modes. Furthermore, inclusion of the sixth peak improves the reduced chi square more effectively than adding other minor contributors, i.e., $d^+$, $d^-(\pi)$, and $r^-$ (Table I). (Comparison of the reduced $\chi^2$ for two versus three and five versus six frequency components clearly shows the importance of the $t$-$d^-$ mode.) The amplitude, frequency and dephasing time of each vibrational mode, as well as the amplitude of the nonresonant term, that were determined from the simultaneous fit of the SFG-FID and spectrum are tabulated in Table II.

The assignment of the sixth peak at 2884 $cm^{-1}$ involves a number of considerations. A band at around 2890 $cm^{-1}$ was observed in bulk alkane crystals by infrared and Raman spectra and was assigned to the Fermi resonance of symmetric $CH_2$ stretching ($d^+_{FR}$) and antisymmetric $CH_2$ stretching ($d^-(0)$), respectively.[44–46] A vibrational mode at, or near, 2884 $cm^{-1}$ has been observed in SFG spectra of surfactants previously.[47] Lu *et al.* observed a peak at around 2884–2908 $cm^{-1}$ in SFG spectra of the air/1-alcohol ($n$=1–8) interface, and assigned it to a $d^-$ mode according to the observed polarization dependence.[48] One source of antisymmetric ($d^-$) modes is gauche defects in the alkyl chain. However, in contrast to the air/1-alcohol interface, where significant gauche defects were identified by observation of a $d^+$ band, our SFG spectrum and SFG-FID showed little evidence of $d^+$ modes suggesting that the ODS molecules are essentially in all-trans conformation. Given the apparent all-trans conformation of the SAM in these experiments, one would expect the $d^-$ (both $\pi$ and 0) mode to be SFG inactive or very weak. Due to a lack of local centrosymmetry, the methylene groups next to either the terminal $CH_3$ group or the anchor moiety, i.e., $Si(\text{-}O\text{-})_3$, can be SFG active even when the alkyl chain has an all-trans conformation. Therefore, a possible assignment for the 2884 $cm^{-1}$ peak is the antisymmetric stretching mode of the terminal $CH_2$ group.

This assignment is consistent with the one previously reported in high resolution SFG and phase sensitive VSFG spectra. Chow *et al.* suggested the presence of a small band at 2886 $cm^{-1}$, assigned to the antisymmetric stretching of the terminal $CH_2$ next to $CH_3$ ($t_2$-$d^-$ or $\omega$-$d^-$), in their high resolution SFG spectra of ODS and Octadecanthiol SAMs.[49] Recently, the Shen group reported a phase sensitive SFG spectrum of ODS, which showed a small negative peak at 2883 $cm^{-1}$, again assigned to $t_2$-$d^-$ mode.[34] Although the symmetric stretching band associated with terminal methylene groups ($t$-$d^+$) was observed in SFG spectrum of a well-packed alkanethiol SAM[50] or alcohol monolayer[51] in all-trans conformation, this band was not detected or resolved in our measurement.

To examine the validity of this assignment, DFT calculations were performed for a simplified model molecule, $CH_3(CH_2)_5Si(OH)_3$ (Table III). The results showed that the $d^-(0)$ type vibrations of methylene groups next to Si ($t_1$-$d^-(0)$) and $CH_3$ ($t_2$-$d^-(0)$), respectively, have nonzero IR intensity at a frequency 30–40 $cm^{-1}$ lower than the $d^-(\pi)$ mode Table II. This is consistent with the assignment of the mode we observe at 2884 $cm^{-1}$. The observation of a strong $d^-(0)$ mode in Raman spectra at around 2880 $cm^{-1}$ (Ref. 46) and the fact that the frequency of the $d^-(\pi)$ mode is known to be in the 2915–2925 $cm^{-1}$ range for $n$-alkyl chains,[52,53] suggest that the observed antisymmetric stretching of terminal methylene groups in our study should be the $t$-$d^-(0)$ mode, which is strongly Raman active[46] and weakly IR active, and not the $t$-$d^-(\pi)$. DFT results confirm that the terminal methylene(s) is the source of the 2884 $cm^{-1}$ peak observed by time- and frequency-domain SFG. However, a rigorous assignment of the 2884 $cm^{-1}$ peak to either $t_1$-$d^-(0)$ or $t_2$-$d^-(0)$ is challenging because the frequencies of the two bands are close to each other. The vibrational modes of the ODS molecule

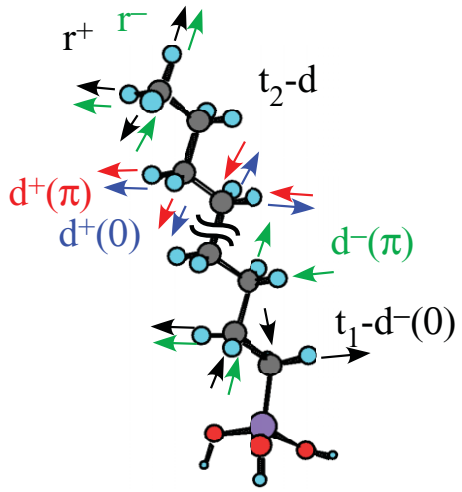


FIG. 5. Schematic drawing of the ODS molecule and the vibrational modes discussed in the text. $d^+(0)$ and $d^-(\pi)$ have the almost same frequency and are unresolved in the spectrum. In the $d^{(+/-)}$ (0) mode, neighboring methylene groups displace in opposite directions while in $d^{(+/-)}(\pi)$, they move in the same direction.

TABLE III. Vibrational frequencies of $CH_3(CH_2)_5Si(OH)_3$ calculated by B3LYP (6-31G(*d*,*p*)) using GAUSSIAN 03. A scaling factor of 0.9614 was used to correct the frequencies (Ref. 55). The $t_1$ and $t_2$ denote terminal methylene next to Si and $CH_3$, respectively. An asterisk (*) denotes that this mode includes motion of $t_2$-$d^-(0)$.

| Frequency ($cm^{-1}$) | Scaled frequency ($cm^{-1}$) | IR Intensity | Assignment |
|---|---|---|---|
| 3008 | 2892 | 1.9 | $d^+(0)$ |
| 3012 | 2896 | 9.6 | $d^+(0)$ |
| 3018 | 2902 | 7.6 | $t_1$-$d^+(0)$ |
| 3024 | 2907 | 48 | $t_2$-$d^+(\pi)$ |
| 3032 | 2915 | 3.4 | $d^-(0)$ |
| 3036 | 2919 | 26 | $d^+(\pi)$ |
| 3037 | 2920 | 72 | $r^+$ |
| 3044 | 2927 | 3.5 | $d^-(0)$* |
| 3056 | 2938 | 8.2 | $t_1$-$d^-$ (0) |
| 3065 | 2947 | 25 | $d^-(\pi)$ |
| 3084 | 2965 | 77 | $d^-$ ($\pi$) |
| 3105 | 2985 | 66 | $r^-$ (op) |
| 3109 | 2989 | 43 | $r^-$ (ip) |

discussed above are illustrated in Fig. 5. Note that this calculation does not include the Fermi resonance, which causes further complexity and frequency shifts of symmetric modes. Antisymmetric stretching modes are not allowed to enter the Fermi resonance interaction[44] so that it is easier to compare the calculated frequency with the experimental value.

### C. Dephasing

The SFG-FID experiments enable the dephasing time of each of the modes contributing to the response to be determined. The dephasing times of the methyl symmetric bands (0.66 ps for $r^+$ and 0.76 ps for $r^+_{FR}$) are in agreement with the range of ones previously reported (0.7 ps for $r^+$ and 1.3 ps for $r^+_{FR}$ of the $O_v$ phase and 1.1 ps for $r^+$ and 0.66 ps for $r^+_{FR}$ of the $L_{2d}$ phase) for the methyl symmetric band of LB films in the liquid condensed phase.[27]

Owing to the relatively large amplitude of the mode at 2884 $cm^{-1}$, $t$-$d^-(0)$, the combination of time and frequency domain SFG data can determine the dephasing time of the $t$-$d^-(0)$ mode with an acceptable error bar. Since, to best of our knowledge, this is the first direct observation of the dephasing ($T_2$) of a terminal $CH_2$ vibration in a SAM, we compare the dephasing of $t$-$d^-(0)$ with that of methylene modes ($d$) observed previously. The $T_2$ of the $d^-(\pi)$ modes of an LB film in an ordered (high density) super-liquid phase and a disordered (and less dense) lower pressure mesophase were found to be 1.04 and 0.18 ps, respectively.[27] The $T_2$ of the bulk $CH_2$ stretching has been reported to be ~1 ps for averaged dephasing of symmetric and antisymmetric $CH_2$ stretching of liquid cyclohexane by time domain coherent anti-stokes Raman spectroscopy.[54] The spectral widths of the $d^-(0)$ mode of bulk $n$-$C_{36}H_{74}$ in Raman spectra have been reported to be 7–9 $cm^{-1}$ in a crystalline phase and 25 $cm^{-1}$ in the liquid phase.[44] Assuming homogeneous broadening, the corresponding $T_2$ of $d^-(0)$ is estimated to be 1.5–1.18 ps in the crystalline phase and 0.42 ps in the liquid phase. These previous studies suggest that $CH_2$ vibrations are sensitive to local order of the alkyl chains, i.e., faster dephasing correlates with increased disorder. The identification of the $t$-$d^-(0)$ mode sheds light on the relatively long dephasing time of this mode (~1.3 ps) and how this dephasing correlates with the structure of the ODS SAMs.

The $T_2$ or 2$\Gamma$ (FWHM) of the $t$-$d^-(0)$ of the ODS SAM (~1.3 ps / 8 $cm^{-1}$) is close to the $T_2$ of the $d^-(0)$ mode of the bulk $n$-$C_{36}H_{74}$ in the crystalline phase.[44] The $T_2$ values measured for the $t$-$d^-(0)$ and the $r^+$ / $r^+_{FR}$ modes suggest that the alkyl chains of the ODS SAM are in an ordered phase but not a perfect crystalline phase, i.e., the structure is similar to the liquid condensed phase of LB.[27] This is consistent with the small (but nonzero) amplitude of the $d^+$ and $d^-$ modes in the SFG spectrum and SFG-FID, which suggests mostly but not completely all-trans configuration of the alkyl chain in the SAM.

## IV. CONCLUSION

We have measured the SFG-FID and SFG spectrum of an ODS SAM on a fused silica substrate. The simultaneous fit of the SFG-FID and the spectrum show that at least six C-H stretching modes are involved in the vibrational response in the 2800–3000 $cm^{-1}$ region. Furthermore, the coherence time of each of these modes, some of which are longer than one picosecond, is determined. The combination of the SFG-FID and the spectrum clearly reveals the presence of a mode at around 2884 $cm^{-1}$ for the all-trans conformation ODS SAMs. This mode is assigned to a 0 type (i.e., neighboring methylene groups displacing in opposite directions) antisymmetric stretching mode of the terminal methylene group. Our experiments measure the dephasing time of the $t$-$d^-(0)$ mode for the first time, to our knowledge. The dephasing time (~1.3 ps) of the $t$-$d^-(0)$ mode implies a liquid condensed phase structure of the alkyl chain which is consistent with the small amplitude of $d^+$ and $d^-$ modes in the SFG spectrum.

## ACKNOWLEDGMENTS

This work was supported by National Science Foundation (CHE 0809838). S.N. acknowledges Dr. Ohe for his useful comments. The advice of Dr. Stan Smith and Dr. Kurt Kistler for the DFT calculations is gratefully acknowledged.

[1] A. Ulman, Chem. Rev. **96**, 1533 (1996).
[2] J. Lee, B. J. Jung, J. I. Lee, H. Y. Chu, L. M. Do, and H. K. Shim, J. Mater. Chem. **12**, 3494 (2002).
[3] P. K. H. Ho, J. S. Kim, J. H. Burroughes, H. Becker, S. F. Y. Li, T. M. Brown, F. Cacialli, and R. H. Friend, Nature **404**, 481 (2000).
[4] C. Joachim, J. K. Gimzewski, and A. Aviram, Nature **408**, 541 (2000).
[5] D. Vuillaume and S. Lenfant, Microelectron. Eng. **70**, 539 (2003).
[6] Y. R. Shen, *The Principles of Nonlinear Optics* (Wiley, New York, 1984).
[7] K. B. Eisenthal, Chem. Rev. **96**, 1343 (1996).
[8] Y. R. Shen and V. Ostroverkhov, Chem. Rev. **106**, 1140 (2006).
[9] E. H. G. Backus, A. Eichler, A. W. Kleyn, and M. Bonn, Science **310**, 1790 (2005).
[10] J. A. McGuire and Y. R. Shen, Science **313**, 1945 (2006).
[11] A. Eftekhari-Bafrooei and E. Borguet, J. Am. Chem. Soc. **131**, 12034 (2009).

[12]A. Eftekhari-Bafrooei and E. Borguet, J. Am. Chem. Soc. **132**, 3756 (2010).
[13]Y. R. Shen, in *Laser Spectroscopy and Photochemistry on Metal Surfaces*, edited by H.-L. Dai and W. Ho (World Scientific, Singapore, 1995).
[14]C. D. Bain, J. Chem. Soc. Faraday Trans. **91**, 1281 (1995).
[15]D. E. Gragson and G. L. Richmond, J. Phys. Chem. B **102**, 3847 (1998).
[16]P. B. Miranda and Y. R. Shen, J. Phys. Chem. B **103**, 3292 (1999).
[17]J. Holman, P. B. Davies, T. Nishida, S. Ye, and D. J. Neivandt, J. Phys. Chem. B **109**, 18723 (2005).
[18]Y. R. Shen, Nature **337**, 519 (1989).
[19]W. Derbyshire, M. van den Bosch, D. van Dusschoten, W. MacNaughtan, I. A. Farhat, M. A. Hemminga, and J. R. Mitchell, J. Magn. Resonance **168**, 278 (2004).
[20]M. H. Rakowsky, K. M. More, A. V. Kulikov, G. R. Eaton, and S. S. Eaton, J. Am. Chem. Soc. **117**, 2049 (1995).
[21]P. Guyot-Sionnest, Phys. Rev. Lett. **66**, 1489 (1991).
[22]J. C. Owrutsky, J. P. Culver, M. Li, Y. R. Kim, M. J. Sarisky, M. S. Yeganeh, A. G. Yodh, and R. M. Hochstrasser, J. Chem. Phys. **97**, 4421 (1992).
[23]J. P. R. Symonds, H. Arnolds, V. L. Zhang, K. Fukutani, and D. A. King, J. Chem. Phys. **120**, 7158 (2004).
[24]W. G. Roeterdink, O. Berg, and M. Bonn, J. Chem. Phys. **121**, 10174 (2004).
[25]C. Hess, M. Wolf, S. Roke, and M. Bonn, Surf. Sci. **502**, 304 (2002).
[26]D. Star, T. Kikteva, and G. W. Leach, J. Chem. Phys. **111**, 14 (1999).
[27]A. N. Bordenyuk, H. Jayathilake, and A. V. Benderskii, J. Phys. Chem. B **109**, 15941 (2005).
[28]A. S. Lagutchev, K. J. Song, J. Y. Huang, P. K. Yang, and T. J. Chuang, Chem. Phys. **226**, 337 (1998).
[29]T. Ye, D. Wynn, R. Dudek, and E. Borguet, Langmuir **17**, 4497 (2001).
[30]S. Nihonyanagi, A. Eftekhari-Bafrooei, J. Hines, and E. Borguet, Langmuir **24**, 5161 (2008).
[31]L. J. Richter, T. P. Petralli-Mallow, and J. C. Stephenson, Opt. Lett. **23**, 1594 (1998).
[32]J. A. McGuire, W. Beck, X. Wei, and Y.-R. Shen, Opt. Lett. **24**, 1877 (1999).
[33]Q. Du, R. Superfine, E. Freysz, and Y. R. Shen, Phys. Rev. Lett. **70**, 2313 (1993).
[34]N. Ji, V. Ostroverkhov, C. Y. Chen, and Y. R. Shen, J. Am. Chem. Soc. **129**, 10056 (2007).
[35]S. Nihonyanagi, S. Yamaguchi, and T. Tahara, J. Chem. Phys. **130**, 204704 (2009).
[36]A. N. Bordenyuk and A. V. Benderskii, J. Chem. Phys. **122** (2005).
[37]T. Mii and H. Ueba, Surf. Sci. **427-428**, 324 (1999).
[38]H. Ueba, T. Sawabu, and T. Mii, Surf. Sci. **502-503**, 254 (2002).
[39]S. Roke, A. W. Kleyn, and M. Bonn, Surf. Sci. **593**, 79 (2005).
[40]M. D. Porter, T. B. Bright, D. L. Allara, and C. E. D. Chidsey, J. Am. Chem. Soc. **109**, 3559 (1987).
[41]S. Ye, S. Nihonyanagi, and K. Uosaki, Phys. Chem. Chem. Phys. **3**, 3463 (2001).
[42]P. Guyot-Sionnest, R. Superfine, J. H. Hunt, and Y. R. Shen, Chem. Phys. Lett. **144**, 1 (1988).
[43]J. Lobau, K. Wolfrum, A. Romphorst, K. Galla, and S. Seeger, Thin Solid Films **289**, 272 (1996).
[44]R. G. Snyder, S. L. Hsu, and S. Krimm, Spectrochim. Acta A **34**, 395 (1978).
[45]I. R. Hill and I. W. Levin, J. Chem. Phys. **70**, 842 (1979).
[46]R. G. Snyder and J. R. Scherer, J. Chem. Phys. **71**, 3221 (1979).
[47]J. C. Conboy, M. C. Messmer, and G. L. Richmond, J. Phys. Chem. B **101**, 6724 (1997).
[48]R. Lu, W. Gan, B. H. Wu, Z. Zhang, Y. Guo, and H. F. Wang, J. Phys. Chem. B **109**, 14118 (2005).
[49]B. C. Chow, T. T. Ehler, and T. E. Furtak, Appl. Phys. B: Lasers Opt. **74**, 395 (2002).
[50]M. Himmelhaus, F. Eisert, M. Buck, and M. Grunze, J. Phys. Chem. B **104**, 576 (2000).
[51]S. R. Goates, D. A. Schofield, and C. D. Bain, Langmuir **15**, 1400 (1999).
[52]R. A. Macphail, H. L. Strauss, R. G. Snyder, and C. A. Elliger, J. Phys. Chem. **88**, 334 (1984).
[53]M. M. Walczak, C. Chang, S. M. Stole, C. A. Widrig, and M. D. Porter, J. Am. Chem. Soc. **113**, 2370 (1991).
[54]H. Kano and H. Hamaguchi, Appl. Phys. Lett. **85**, 4298 (2004).
[55]M. P. Andersson and P. Uvdal, J. Phys. Chem. A **109**, 2937 (2005).